PENETRATIVE CONVECTION

G. VERONIS
Woods Hole Oceanographic Institution

Received January 27, 1962; revised August 23, 1962

ABSTRACT

The bottom of a layer of water is maintained at 0° C and the top at a temperature greater than 4° C. Thus a gravitationally unstable layer of fluid lies below a layer which is stably stratified. When convection occurs in the lower layer, the motions will penetrate into the upper layer. This system is analyzed to determine the extent of the penetration into the stable fluid. The perturbation method employed in the present paper is a modification of the technique discussed in an earlier paper and is applicable to a system in which the infinitesimal motions can be deduced only approximately. The results indicate that the system can become unstable to a finite amplitude disturbance at values of the Rayleigh number less than the critical value of infinitesimal stability theory. A simple physical explanation is put forth to explain the occurrence of a finite amplitude instability. Experimental efforts by Furumoto and Rooth (unpublished) have not been successful in determining whether or not a finite amplitude instability occurs.

I. INTRODUCTION

In natural phenomena the process of thermal convection ordinarily involves penetration into a stably stratified fluid. Examples of this penetrative convection can be cited in several of the areas of study of geophysical fluid dynamics. The atmosphere is bounded below by the ground or the ocean, and, as these bounding surfaces are heated by solar radiation, the air near the surface becomes warmer than the upper air and therefore gravitationally unstable. When convection occurs, the warm air is carried aloft into regions which are stably stratified. In the oceans evaporation is the primary physical process which gives rise to gravitational instability near the surface. As the cool surface water is carried downward, it also enters regions that are stably stratified. In both meteorology and oceanography the extent to which convective motions penetrate into the bounding stable fluid is difficult to determine because the stability of the latter is determined by large-scale dynamical processes. Thus the study of penetrative convection is coupled with that of the general circulation of the entire fluid system, and any analysis of the penetration must either incorporate the large-scale processes as part of the analysis or take these processes into account by some assumed parametric representation.

Penetrative convection in stars can, for the most part, be decoupled from other circulation processes. Here the surface layer is stable. At some distance below the "surface" the increase in temperature due to adiabatic compression causes negative hydrogen to form and the latter is opaque to photons. The temperature gradient therefore rises to a value greater than the adiabatic gradient and the region is unstable. Depending on the type of star, this superadiabatic gradient can extend far into the interior to a point where the very high temperature causes the gas to become completely ionized and the gradient no longer is superadiabatic. An unstable layer is formed, therefore, with stable fluid both above and below. Although the static state is determined by molecular processes alone, the analysis is complicated by the introduction of radiative processes into the energy equation, as well as by large variations in temperature, density, and pressure.

It is desirable to isolate the phenomenon of penetrative convection to a system which is free of the difficulties encountered in the natural phenomena mentioned above. This isolation can be effected by any one of three laboratory experiments.

The first (and the one treated in this paper) is an experiment with a layer of water with boundary temperatures of 0° C at the lower boundary and >4° C at the upper boundary. In the static state the temperature gradient is constant, and the layer of maximum density is at the 4° C level. The fluid below the 4° C level is gravitationally unstable; the fluid above is stable. When convection occurs in the lower region, the motions will penetrate into the stable fluid. This experiment is being performed by A. Furumoto and C. Rooth at the Woods Hole Oceanographic Institution.

The second experiment, presently being carried out by A. Faller of the Woods Hole Oceanographic Institution, is a quasi-steady one in which a layer of air is bounded by two horizontally flat boundaries which are maintained at horizontally uniform temperatures. The boundary temperatures are steadily increased or decreased with time. Because of the finite conductivity of air, the temperature at an interior point of the fluid lags behind the boundary value, and two layers—one gravitationally stable, the other unstable—are formed. When convection occurs, the motions of the unstable layer penetrate into the stable layer.

The third experiment is not a thermal experiment but, instead, involves the destabilizing effect of centrifugal forces when two concentric cylinders are rotated in opposite directions (the familiar Taylor experiment [1923]). The rotation of the inner cylinder causes the adjacent fluid to become unstable and to move toward the outer cylinder. The rotation of the latter creates a stable cylinder of fluid into which the unstable flow will penetrate.[1]

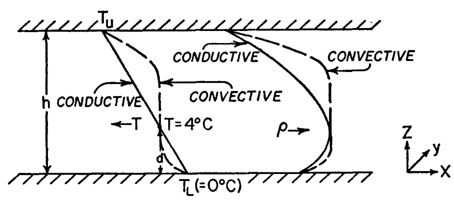

FIG. 1.—A layer of water is bounded by two surfaces with temperatures 0° C at the lower boundary ($z = 0$) and >4° C at the upper boundary ($z = h$) The depth of the 4° C layer in the conductive state is denoted by $d(< h)$. The linear temperature profile corresponds to the conductive state; the curved (*dashed*) temperature profile is a schematic picture of the horizontally averaged profile when convection is present. The density profiles are shown in the right side of the figure.

Of the three experiments, the first is probably the simplest to carry out in the laboratory. The basic variable to be measured is the temperature, which is considerably simpler to determine than is the azimuthal velocity in the moving system of oppositely rotating cylinders. Also the steady-state character of the experiment is a definite advantage over the quasi-steady-state experiment. We shall therefore confine our attention to the first experiment. A schematic diagram of the system is shown in Figure 1. The static density and temperature profiles are denoted by "conductive." After convection has set in, the horizontally averaged profiles are distorted to shapes which are sketched in and called "convective."

According to Furumoto and Rooth, the convective state involves a very broad region of water with temperature at or slightly below 4° C. The fluid near the upper boundary has a linear vertical temperature gradient which is essentially uniform horizontally. In the convective region there are (Bénard) cellular-like motions, and, for the experiments where the temperature at the upper plate was between 12° and 20° C, observations of the vertical structure indicate that more than one cell exists. Near the cold bottom plate the motion is considerably weaker, and the horizontally averaged vertical temperature gradient has the same value as that of the fluid near the upper boundary.

Furumoto and Rooth have obtained limited quantitative measurements of some of the variables. In the plot of vertical heat transport, H, versus Rayleigh number, R (see eq. [25] for definition), it appears that a curve given by $H \sim R^{1/3}$ can be drawn through

[1] The analogy between the water problem described above and the flow between two cylinders of opposite rotation was first pointed out to me by W. V. R. Malkus, who also encouraged Furumoto and Rooth to conduct the experiment.

the available data in the entire convective range. This is the form of the asymptotic law for large Rayleigh number in the ordinary (Bénard) convection experiment of a fluid heated from below and cooled from above. The fact that it holds even for slightly supercritical values in the present experiment is surprising because the $H \sim R^{1/3}$ law is associated with fully turbulent Bénard convection.

A second anomalous feature of this experiment which may have some bearing on the validity of the $H \sim R^{1/3}$ law for small R is the possibility of the growth of a finite amplitude disturbance at a value of the Rayleigh number smaller than the critical value which is derived from linear stability theory.[2] One can give a simple physical argument for the occurrence of a finite amplitude instability. In the static state the density, ρ, has a maximum at the 4° C level, and the equation of state is essentially parabolic about the 4° C point, i.e., $\rho = \rho_0(1 - \alpha T^2)$, where T is the deviation of the temperature from 4° C and ρ_0 is the density of 4° C water. Any process which tends to mix water of, say, 3° and 5° C generates 4° C water. This mixing creates water with maximum density throughout a layer of large thickness. If a finite amplitude disturbance were capable of effecting this mixing of water, it would generate a gravitationally unstable layer which would be deeper than the corresponding layer in the conductive state. Hence a finite amplitude instability could result if large-amplitude noise were available. It is possible that this finite amplitude instability could occur at values of the Rayleigh number considerably smaller than the critical value according to linear theory. In such a case, large-amplitude, subcritical motions would result. Furthermore, the convective process tends to create a deep layer of water with a horizontally averaged temperature close to 4°. However, this type of regime with sharp boundary gradients and a deep isothermal region is characteristic of fully turbulent flow. Hence one might expect the $H \sim R^{1/3}$ law to hold for moderate Rayleigh numbers.

In the analysis which follows it is shown that a finite amplitude instability is possible for an experiment where the boundaries are idealized to "slip" or "free" boundaries. (There is no reason to expect that this conclusion would be altered by a rigid boundary analysis.) The solution of the finite amplitude problem is pivoted about the linear stability analysis. Because the results indicate a subcritical instability, the second-order solution can give no verifiable results of heat transport versus Rayleigh number. The H versus R relation, which might be observable experimentally, requires extension of the present analysis to the fourth or preferably the sixth order.

The physical problem which is treated here leads to a mathematical problem for which exact solutions have not been found even in the stability analysis. The stability analysis can be handled approximately without too much difficulty by applying the Fourier series approach which Jeffreys and Jeffreys (1946) describe for treating the rigid-boundary Bénard problem. However, the finite amplitude problem cannot be solved by the method proposed by Malkus and Veronis (1958). The reason for this departure from the previously established approach is that the stability problem about which the finite amplitude solution is pivoted has been solved by using approximate eigenfunctions. In the iterative procedure for the finite amplitude solution the small errors in the stability analysis mount up, and considerably larger errors result even in the second order when the method of Malkus and Veronis is used.

II. EQUATIONS FOR PENETRATIVE CONVECTION

The appropriate equations for the study of the finite amplitude problem are the Boussinesq form of the Navier-Stokes equations and the heat equation:

$$\frac{\partial \boldsymbol{v}}{\partial t} + \boldsymbol{v} \cdot \nabla \boldsymbol{v} = -\frac{1}{\rho_0} \nabla p - \frac{g\rho}{\rho_0} \boldsymbol{k} + \nu \nabla^2 \boldsymbol{v}, \tag{1}$$

[2] We shall refer to such values of R as "subcritical."

$$\nabla \cdot v = 0 \,, \tag{2}$$

$$\frac{\partial T}{\partial t} + v \cdot \nabla T = k \nabla^2 T \,. \tag{3}$$

In the vicinity of the 4° C point the equation of state can be adequately represented by the quadratic form[3]

$$\rho = \rho_0 [1 - \alpha (T - T_0)^2] \,, \tag{4}$$

where $T_0 = 4°$ C, $\alpha \approx 7.68 \times 10^{-6}/(° \text{C})^2$, and ρ_0 is the density at 4° C. Equation (4) is very accurate near the 4° C point and involves a 10 per cent error at 14° C. In the experiment, however, water of higher temperature is in the stable region, and one may anticipate that errors in the equation of state for higher temperatures affect the results negligibly.

Substituting equation (4) in equation (1) yields

$$\frac{\partial v}{\partial t} + v \cdot \nabla v = -\frac{1}{\rho_0} \nabla p - g [1 - \alpha (T - T_0)^2] k + \nu \nabla^2 v \,. \tag{5}$$

It is convenient in the subsequent development to divide the temperature into a mean and a fluctuating value, where the mean corresponds to a horizontal average and is a function of z alone in the steady-state experiment. Thus, denoting the horizontal average by a bar or by an angular bracket, we have

$$T = \bar{T}(z) + T(x, y, z, t) \,, \tag{6}$$

where, by definition, $\langle T(x, y, z, t) \rangle \equiv 0$.

A horizontal average of equation (3) gives the equation for the mean temperature,

$$-\kappa \frac{d^2 \bar{T}}{d z^2} + \frac{d}{d z} (\langle w T \rangle) = 0 \,, \tag{7}$$

or, upon integration with respect to z,

$$-\kappa \frac{d \bar{T}}{d z} + \langle w T \rangle = H = \text{Const.} \,, \tag{8}$$

where H is the vertical kinematic heat flux (downward in this problem). A vertical average of equation (8) produces another equation for H:

$$-\kappa \frac{\Delta T}{d} + (w T)_m = H \,, \tag{9}$$

where $(wT)_m$ means an average over the entire fluid. In equation (9) $\Delta T \equiv 4°$ C and d is the height of the 4° C layer above the bottom boundary so that $\Delta T/d$ is the (constant) temperature gradient when only conduction occurs.

From equations (8) and (9) we derive the following relation between the mean gradient and the fluctuation quantities w and T:

$$\kappa \frac{d \bar{T}}{d z} = \kappa \frac{\Delta T}{d} + \langle w T \rangle - (w T)_m \,. \tag{10}$$

[3] In tables of physical constants the equation for the density of water at atmospheric pressure as a function of temperature is given as a polynomial in T with 0° C as reference temperature. When 4° C is used as reference temperature, α has the value given here.

This can be integrated to yield

$$\bar{T}-T_0=-\Delta T+\left(\frac{\Delta T}{d}-\frac{(wT)_m}{\kappa}\right)z+\frac{1}{\kappa}\int_0^z\langle wT\rangle dz\,. \tag{11}$$

We substitute equation (6) into equation (5) and incorporate the mean part of the temperature into the pressure (total term denoted by $\tilde{p}$) to arrive at

$$\frac{\partial \boldsymbol{v}}{\partial t}+\boldsymbol{v}\cdot\nabla\boldsymbol{v}=-\frac{1}{\rho_0}\nabla\tilde{p}+[2g\alpha(\bar{T}-T_0)T+g\alpha T^2]\boldsymbol{k}+\nu\nabla^2\boldsymbol{v}\,. \tag{12}$$

We take the z component of $\nabla\times\nabla\times$ (eq. [12]) and use equation (2) to eliminate the horizontal velocities u and v in the linear terms and finally have

$$\left(\frac{\partial}{\partial t}-\nu\nabla^2\right)\nabla^2 w=2g\alpha(\bar{T}-T_0)\nabla_1^2 T+g\alpha\nabla_1^2 T^2+L\,, \tag{13}$$

where

$$\nabla_1^2=\frac{\partial^2}{\partial x^2}+\frac{\partial^2}{\partial y^2}\qquad\text{and}\qquad L\equiv\frac{\partial}{\partial z}\left[\frac{\partial}{\partial x}(\boldsymbol{v}\cdot\nabla u)+\frac{\partial}{\partial y}(\boldsymbol{v}\cdot\nabla v)\right]-\nabla_1^2(\boldsymbol{v}\cdot\nabla w)\,.$$

Subtracting equation (7) from equation (3) yields

$$\frac{\partial T}{\partial t}-\kappa\nabla^2 T=-\frac{\partial\bar{T}}{\partial z}w-h\,, \tag{14}$$

where $h=\boldsymbol{v}\cdot\nabla T-(\partial/\partial z)(\langle wT\rangle)$.

We can eliminate the pressure from the horizontal equations of motion and make use of the continuity equation to relate the horizontal velocity components to the vertical velocity in the linear terms. Thus

$$\left(\frac{\partial}{\partial t}-\nu\nabla^2\right)\left(\nabla_1^2 u+\frac{\partial^2 w}{\partial x\partial z}\right)=\frac{\partial^2}{\partial x\partial y}(\boldsymbol{v}\cdot\nabla v)-\frac{\partial^2}{\partial y^2}(\boldsymbol{v}\cdot\nabla u)\,, \tag{15}$$

$$\left(\frac{\partial}{\partial t}-\nu\nabla^2\right)\left(\nabla_1^2 v+\frac{\partial^2 w}{\partial y\partial z}\right)=\frac{\partial^2}{\partial x\partial y}(\boldsymbol{v}\cdot\nabla u)-\frac{\partial^2}{\partial x^2}(\boldsymbol{v}\cdot\nabla v)\,. \tag{16}$$

The boundary conditions at $z=0$ and $z=h$ are given by

$$u=v=w=0\qquad\text{for rigid boundaries}\,, \tag{17a}$$

$$\frac{\partial u}{\partial z}=\frac{\partial v}{\partial z}=w=0\qquad\text{for free boundaries}\,, \tag{17b}$$

and, since we consider the boundary temperature fixed,

$$T=0\quad\text{at}\quad z=0,\quad z=h\,. \tag{18}$$

Equations (13)–(18) form the fundamental set of equations for the analysis. For the subsequent development we find it convenient to non-dimensionalize the equations in the following fashion. Write

$$\boldsymbol{r}=h\boldsymbol{r}'\,,\quad \boldsymbol{v}=\frac{\kappa}{h}\boldsymbol{v}'\,,\quad T=\frac{\nu\kappa}{2h^3 g\alpha\Delta T}T'\,,\quad t=\frac{d^2}{\kappa}t'\,,\quad \sigma=\frac{\nu}{\kappa}\,,\quad \lambda=\frac{h}{d}\,, \tag{19}$$

and $R = [2d^3 g\alpha(\Delta T)^2/\kappa\nu]\lambda^4$. Then equations (13)–(16) can be written as (all primes are dropped and the variables are now non-dimensional)

$$\left(\frac{1}{\sigma}\frac{\partial}{\partial t}-\nabla^2\right)\nabla^2 w = -\left[(1-\lambda z)+\lambda\frac{(wT)_m}{R}z-\frac{\lambda}{R}\int_0^z\langle wT\rangle dz\right] \times\nabla_1^2 T-\frac{\lambda}{2R}\nabla_1^2 T^2-\frac{1}{\sigma}L, \tag{20}$$

$$\left(\frac{\partial}{\partial t}-\nabla^2\right)T = [R+\langle wT\rangle-(wT)_m]w+h, \tag{21}$$

$$\left(\frac{1}{\sigma}\frac{\partial}{\partial t}-\nabla^2\right)\left(\nabla_1^2 u+\frac{\partial^2 w}{\partial x\partial z}\right)=\frac{1}{\sigma}\left[\frac{\partial^2}{\partial x\partial y}(\boldsymbol{v}\cdot\nabla v)-\frac{\partial^2}{\partial y^2}(\boldsymbol{v}\cdot\nabla u)\right], \tag{22}$$

$$\left(\frac{1}{\sigma}\frac{\partial}{\partial t}-\nabla^2\right)\left(\nabla_1^2 v+\frac{\partial^2 w}{\partial y\partial z}\right)=\frac{1}{\sigma}\left[\frac{\partial^2}{\partial x\partial y}(\boldsymbol{v}\cdot\nabla u)-\frac{\partial^2}{\partial x^2}(\boldsymbol{v}\cdot\nabla v)\right], \tag{23}$$

where the non-dimensional form of equation (11), viz.,

$$\frac{\bar{T}-T_0}{\Delta T} = -1+\lambda\left[1-\frac{1}{R}(wT)_m\right]z+\frac{\lambda}{R}\int_0^z\langle wT\rangle dz, \tag{24}$$

has been used in equation (20).

The non-dimensionalization is straightforward. Either h or d can be used for the length scale and either κ/d or ν/d for the characteristic velocity. The remaining definitions in equations (19) follow almost automatically.

The quantity

$$R = 2\lambda^4\frac{g\alpha(\Delta T)^2}{\kappa\nu}d^3 \equiv 2\lambda^4\frac{g\Delta\rho}{\rho\cdot\kappa\nu}d^3 \tag{25}$$

(where $\Delta\rho$ is the [constant] density difference between 0° and 4° C water) is $2\lambda^4$ times the Rayleigh number for the present problem. To simplify the notation, we incorporate the factor $2\lambda^4$ into R. However, when we speak of the Rayleigh number, it should be understood that the reference is to $R/2\lambda^4$. As in the Bénard problem, the Rayleigh number contains a "potential-energy-releasing" term in the numerator, viz.,

$$g\frac{\alpha(\Delta T)^2}{d}\left(\equiv\frac{g\Delta\rho}{d\rho_0}\right),$$

and the product of two "dissipation" terms in the denominator, viz., κ/d^2 and ν/d^2. Thus an increase in R corresponds to an increase in rate of release of potential energy or a decrease in rate of dissipation—either would tend to destabilize the system.

The method of solution is based on the method proposed by Malkus and Veronis (1958). We expand the velocity and temperature fluctuation in a power series of a small amplitude factor ϵ. The parameter, R, is also expanded in a power series. Thus

$$\begin{aligned} \boldsymbol{v} &= \epsilon\boldsymbol{v}_0+\epsilon^2\boldsymbol{v}_1+\epsilon^3\boldsymbol{v}_2+\ldots, \\ T &= \epsilon T_0+\epsilon^2 T_1+\epsilon^3 T_2+\ldots, \\ R &= R_0+\epsilon R_1+\epsilon^2 R_2+\ldots. \end{aligned} \tag{26}$$

Since the equations can now be expressed in a power series in ϵ and since the coefficients of each power of ϵ must vanish for each equation, we are led to a series of ordered equations in $\boldsymbol{v}_i$, T_i, R_i. The ordered set will not be written here, but each set of equations will be written down as needed.

III. FIRST-ORDER EQUATIONS

Substituting equations (26) in equations (20) and (21), we can write the set of equagions for first-order velocity and temperature fluctuations:

$$\left(\frac{1}{\sigma}\frac{\partial}{\partial t}-\nabla^2\right)\nabla^2 w_0=(1-\lambda z)\nabla_1^2 T_0\,, \tag{27}$$

$$\left(\frac{\partial}{\partial t}-\nabla^2\right)T_0=-R_0 w_0\,. \tag{28}$$

The boundary conditions in terms of the variables w_0 and T_0 can be derived from equations (17), (18), and (2). *We now restrict our attention to stress-free boundaries.* Then

$$\left.\begin{aligned} w_0&=\frac{\partial^2 w_0}{\partial z^2}=0\,,\\ T_0&=0\,,\end{aligned}\right\}\quad z=0,\,1\,. \tag{29}$$

We can eliminate one of the variables T_0 or w_0. In the present case it is more convenient to work with T_0, and we therefore eliminate w_0 from equations (27) and (28), and, using equation (28), we can express the boundary condition (29) in terms of T_0. Thus

$$\left(\frac{1}{\sigma}\frac{\partial}{\partial t}-\nabla^2\right)\left(\frac{\partial}{\partial t}-\nabla^2\right)\nabla^2 T_0=R_0(1-\lambda z)\nabla_1^2 T_0\,, \tag{30}$$

$$T_0=\frac{\partial^2 T_0}{\partial z^2}=\frac{\partial^4 T_0}{\partial z^4}=0 \qquad \text{on} \qquad z=0,\,1\,. \tag{31}$$

Equations (30) and (31) are homogeneous equations in T_0. We are therefore confronted with an eigenvalue problem. In particular, we wish to find the relationship between R_0, σ, and the time and spatial dependence of T_0, which must be satisfied for the basic conductive state to be unstable to infinitesimal disturbances.

We shall assume separability of t, x, y, and z in equation (30). In particular, we assume a form

$$T_0\sim e^{st}f(x,y)T_0(z)\,, \tag{32}$$

where

$$\nabla_1^2 f(x,y)=-a^2 f(x,y)\,, \tag{33}$$

i.e., where T_0 has a cellular structure in the horizontal direction. Then equations (30) and (31) can be written as

$$(D^2-a^2)\left[\frac{s}{\sigma}-(D^2-a^2)\right][s-(D^2-a^2)]T_0=-a^2R_0(1-\lambda z)T_0\,, \tag{34}$$

$$T_0=D^2T_0=D^4T_0=0 \qquad \text{on} \qquad z=0,\,1\,, \tag{35}$$

where $D\equiv d/dz$.

a) Principle of Exchange of Stabilities

It will first be shown that s must be real for undamped disturbances in the free boundary systems,[4] i.e., for marginal stability $s=0$.

Multiply equation (34) by T_0^*, the complex conjugate of T_0, and integrate from $z=0$

[4] This result was originally derived by E. A Spiegel (unpublished) for a system with an arbitrary mean temperature profile. The principle has not been established for rigid boundaries.

to $z = 1$. Then, by integrating by parts, we can show that the resultant equation can be written

$$\frac{s^2}{\sigma}\int_0^1 (DT_0DT_0^* + a^2T_0T_0^*)\,dz$$

$$+\left(\frac{1}{\sigma}+1\right)s\int_0^1 (D^2T_0D^2T_0^* + 2a^2DT_0DT_0^* + a^4T_0T_0^*)\,dz$$

$$+\int_0^1 (D^3T_0D^3T_0^* + 3a^2D^2T_0D^2T_0^* + 3a^4DT_0DT_0^* + a^6T_0T_0^*)\,dz \tag{36}$$

$$= a^2R_0\int_0^1 (1-\lambda z)T_0T_0^*\,dz\,,$$

or

$$s^2I_1 + sI_2 + I_3 = R_0I_4\,, \tag{37}$$

where the I_i's—$i = 1, 2, 3$—are the positive definite coefficients in equation (36).

If we take the complex conjugate of equation (34) and multiply by T_0 and integrate in the vertical, we get

$$s^{*2}I_1 + s^*I_2 + I_3 = R_0I_4\,, \tag{38}$$

where the I_i's are the same as in equation (37).

Write $s = p + iq$, $s^* = p - iq$. Subtracting equation (38) from equation (37) then yields

$$iq[4pI_1 + 2I_2] = 0\,.$$

Hence

$$q = 0 \qquad \text{or} \qquad p = -\frac{I_2}{2I_1}, \tag{39}$$

i.e., for marginal stability ($p = 0$), it is necessary that $q = 0$. The principle of exchange of stabilities is therefore established.

b) Stability Problem

Equation (34) can now be written

$$\mathfrak{L}T_0 \equiv [(D^2 - a^2)^3 + a^2R_0(1 - \lambda z)]T_0 = 0 \tag{40}$$

and is the same equation as that for flow between rotating cylinders. (In the latter problem, λ is interpreted as 1 minus the ratio of the rotation rates of the outer to the inner cylinder.) The boundary conditions given by equations (35) are for free boundaries. Rigid boundary conditions are the same as those for the rotating-cylinder problem (cf. Taylor 1923; Chandrasekhar 1954). As stated earlier, we restrict our attention to free boundaries.[5]

We can represent T_0 by a Fourier sine series in the vertical and derive expressions for the Fourier amplitudes from equation (40). For the free-boundary problem, the Fourier sine series is particularly useful because the boundary conditions are automatically satisfied. Also, derivatives of T_0 up to the sixth order can be represented by the differentiated Fourier series even at the boundary points because of the particular form

[5] L. N. Howard has suggested that the analysis of Jeffreys and Jeffreys (1946) for the Bénard convection problem is particularly appropriate for the present problem when λ is not too large. He has carried out the analysis for the stability problem with a variety of boundary conditions and reproduces the results of Chandrasekhar (for the Taylor rotating-cylinder problem). We apply the same method here for the free-boundary stability problem and use the results for the finite amplitude range.

of the boundary conditions. (The difficulty with convergence at the boundary as discussed by Jeffreys and Jeffreys 1946 does not enter explicitly as it does in the rigid boundary problem. However, the higher-order even derivatives of T_0, e.g., $\partial^8 T_0/\partial z^8$ do not vanish.)

We now introduce two useful definitions for the stability problem. Let

$$a^2 = \pi^2 \alpha^2, \quad \pi z = \zeta . \tag{41}$$

Then equation (40) becomes

$$\left(\frac{d^2}{d\zeta^2} - a^2\right)^3 T_0 = -\alpha^2 R_0' \left(1 - \frac{\lambda \zeta}{\pi}\right) T_0 , \tag{42}$$

where $R_0' = R_0/\pi^4$. Substituting the Fourier series representation,

$$T_0 = \sum_1^{\infty} A_n \sin n\zeta , \tag{43}$$

in equation (42), we derive the expression (after dividing by R_0')

$$\frac{1}{R_0'} \sum_1^{\infty} (n^2 + a^2)^3 A_n \sin n\zeta = \left(1 - \frac{\lambda \zeta}{\pi}\right) a^2 \sum_1^{\infty} A_n \sin n\zeta . \tag{44}$$

Now multiply by $\sin r\zeta$ and integrate from $\zeta = 0$ to $\zeta = 1$ to get

$$\begin{aligned} &\text{Odd } r: \frac{\pi^2}{2}\left[a^2 - \frac{(r^2+a^2)^3}{R_0'}\right] A_r = a^2 \lambda \left[\frac{\pi^2}{4} A_r - \sum_{\text{even } n} \frac{4rn}{(r^2-n^2)^2} A_n\right], \\ &\text{Even } r: \frac{\pi^2}{2}\left[a^2 - \frac{(r^2+a^2)^3}{R_0'}\right] A_r = a^2 \lambda \left[\frac{\pi^2}{4} A_r - \sum_{\text{odd } n} \frac{4rn}{(r^2-n^2)^2} A_n\right]. \end{aligned} \tag{45}$$

Expression (45) represents an infinite matrix relating the various Fourier amplitudes. Since the equations are homogeneous, it is necessary that some condition (expressed as a determinant of the coefficients of the A_i) between R_0, λ, and a be satisfied in order to make the system of equations consistent. We shall consider several different values of λ corresponding to different temperatures for the upper boundary. In each case the matrix will be truncated and an approximate relation between R_0, λ, and a will be derived.

The general determinant formed from equation (45) is

$$\begin{vmatrix} \left(1-\frac{\lambda}{2}\right)\beta_1 - \frac{1}{R_0'} & \lambda \frac{16}{9\pi^2}\beta_1 & 0 & \lambda\frac{32}{225\pi^2}\beta_1 & \cdots \\ \lambda\frac{16}{9\pi^2}\beta_2 & \left(1-\frac{\lambda}{2}\right)\beta_2 - \frac{1}{R_0'} & \lambda\frac{48}{25\pi^2}\beta_2 & 0 & \cdots \\ 0 & \lambda\frac{48}{25\pi^2}\beta_3 & \left(1-\frac{\lambda}{2}\right)\beta_3 - \frac{1}{R_0'} & \lambda\frac{96}{49\pi^2}\beta_3 & \cdots \\ \lambda\frac{32}{225\pi^2}\beta_4 & 0 & \lambda\frac{96}{49\pi^2}\beta_4 & \left(1-\frac{\lambda}{2}\right)\beta_4 - \frac{1}{R_0'} & \cdots \\ \cdots & \cdots & \cdots & \cdots & \end{vmatrix} = 0 , \tag{46}$$

where

$$\beta_r = \frac{a^2}{(r^2 + a^2)^3}.$$

Case I: $T = 4°$ C at $z = h$; $\lambda = 1$.—For this case, just the first term is sufficient because the determinant yields the minimum R_0 with surprising accuracy.

$$\frac{R_0}{2\lambda^4} = 6.75\pi^4 \qquad \text{for} \qquad a^2 = 0.5\,. \tag{47a}$$

The 4×4 determinant gives

$$\frac{R_0}{2\lambda^4} = 6.72\pi^4 \qquad \text{for} \qquad a^2 = 0.507\,. \tag{47b}$$

The present result can be derived even more simply if one notes that, since the entire layer is unstable, the destabilizing term on the right-hand side of the stability equation,

$$\left(\frac{d^2}{dz^2} - \pi^2 a^2\right)^3 T_0 = -\pi^2 a^2 R_0'(1 - z) T_0\,,$$

can be approximated by its average value $-(\pi^2 a^2/z) R_0' T_0$. Then $\sin \pi z$ is the exact eigenfunction of the approximate problem and one obtains equation (47*a*) as the result.

It is worthwhile to pause at this point and compare the results with those of Rayleigh for the Bénard problem, viz.,

$$R_0 = 6.75\pi^4 \quad \text{for} \quad a^2 = 0.5\,.$$

It is seen that the Rayleigh number is identical with the value given by equation (47*a*). The larger mass of dense water at the top of the layer tends to make the system more unstable gravitationally than the Bénard system. However, the depth over which the density gradient is appreciable is smaller in the present problem. This appears as a stabilizing effect and just compensates for the destabilizing effect of the deeper layer of dense water. This result should be kept in mind in the remaining cases where the addition of the stable layer will add an additional degree of freedom, viz., the boundary condition at the top of the unstable layer is relaxed so that the fluid motion can penetrate into the stable layer and seek its optimum form.

Case II: $T = 8°$ C at $z = h$; $\lambda = 2$.—The 2×2 determinant suffices and is equivalent to the equation

$$R_0 = \frac{9\pi^6}{16\lambda} \frac{(1 + a^2)^{3/2}(4 + a^2)^{3/2}}{a^2}, \tag{48}$$

which, when minimized with respect to a^2, yields

$$\frac{R_0}{2\lambda^4} = 2.73\pi^4 \qquad \text{for} \qquad \frac{a^2}{\lambda^2} = \frac{-5 + \sqrt{153}}{32} \approx 0.230\,. \tag{49}$$

The 4×4 determinant gives the slightly altered result,

$$\frac{R_0}{2\lambda^4} = 2.72\pi^4 \qquad \text{for} \qquad \frac{a^2}{\lambda_2} = 0.234\,. \tag{50}$$

In order to make a comparison with the Bénard problem, we have divided a^2 by λ^2, since this changes the meaning of a to the wave number defined on the basis of the depth of the unstable layer. Thus the addition of the stable layer has relaxed the constraints to such a degree that the Rayleigh number is decreased to less than half the value of the Bénard problem and of Case I, and the scale has increased by about 50 per cent ($a/\lambda = 0.48$ as compared with $a/\lambda = 0.71$ in Bénard convection).

We shall concentrate on Case II in the finite amplitude analysis and shall make use of the relatively simple results of the 2×2 matrix. Using equation (48) in the truncated 2×2 determinant (46), we find, for the coefficients of sin ζ,

$$\frac{A_1}{A_2} = 4.1 ; \qquad A_r = 0 , \qquad r > 2 . \tag{51}$$

The corresponding w_0 expression can be derived from equation (28) with $\partial T_0/\partial T = 0$. Graphs of w_0 versus z and T_0 versus z are given in Figure 2. Note that there is a small reversed cell at the top of the layer of fluid.

The remaining cases are listed in Table 1. They were derived by using the 4×4 truncated matrix so that the results were carried only up to $\lambda = 3.5$. For higher λ, one should go to a truncated matrix of higher order for equivalent accuracy (≥ 99 per cent).

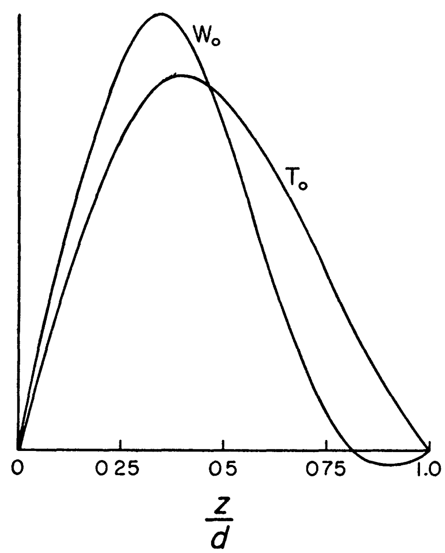

FIG. 2.—A plot of w_0 versus z for $\lambda = 2$ with T_0 normalized, i.e., $(T_0)_m = 1$, and w_0 deduced from eq. (28) A small secondary cell near the upper boundary is driven by viscous forces and is shown as the region in which w_0 is negative.

TABLE 1

CRITICAL RAYLEIGH NUMBERS AND CORRESPONDING WAVE NUMBERS FOR VARIOUS VALUES OF λ IN STRESS-FREE PROBLEM

λ	a^2	R_0/π^4	a^2/λ^2	$R_0/2\lambda^4\pi^4$
0 .	0 500	6 75	. .	. .
1 0	0 500	13 43	0 5	6 72
1 2	0 505	16 69	351	4 03
1 4	0 519	21 92	265	2 81
1 6	0 535	31 37	209	2 40
1 8	0 630	50 86	194	2 42
1 9	0 750	67 07	205	2 58
2 0	0 930	87 18	233	2 73
2 5	1 64	222 2	.262	2 84
3 0	2 29	547 9	254	2 83
3 5	3 10	854 7	0 253	2 84

The results for the problem with rigid boundaries are listed in Table 2. The second and third columns are the results of Chandrasekhar (1954) and were taken from Chandrasekhar's book (1961), in which he presents the values of the critical Taylor number, T_c, and the corresponding wave numbers a for Couette flow. It was noted earlier that the stability problem for rigid boundaries is identical with the Couette flow problem solved by Chandrasekhar. His values of a in the second column were squared and divided by $(1-\mu)^2\pi^2(\equiv\lambda^2\pi^2)$ (μ is the ratio of rotation rates of outer to inner cylinder) and the values $a^2/(1-\mu)^2\pi^2$ can be compared with the values α^2/λ^2 in Table 1. His values of the critical Taylor number, T_c, were divided by $2(1-\mu)^2\pi^4(\equiv 2\lambda^4\pi^4)$ for comparison with $R_0/2\lambda^4\pi^4$ in Table 1.

There is, of course, a quantitative difference between the results of the two cases because of the different boundary conditions. However, the qualitative behavior is the same, and we shall therefore discuss the stress-free problem only.

There are several interesting features evident from an inspection of Table 1. The modified wave number α/λ has a minimum value at about $\lambda = 1.8$, then rises to a local

TABLE 2*

CRITICAL RAYLEIGH NUMBERS AND CORRESPONDING WAVE NUMBERS FOR VARIOUS VALUES OF λ IN RIGID-BOUNDARY PROBLEM

$1-\mu(\equiv\lambda)$	a	T_0	$a^2/(1-\mu)^2\pi^2$	$T_0/2(1-\mu)^2\pi^4$
0	3 12	$1\ 708\times10^3$	. . . .	. . . .
1 .	3 12	$3\ 390\times10^3$	0 986	17 40
1 25	3 13	$4\ 462\times10^3$	635	9 383
1 5	3 20	$6\ 417\times10^3$	461	6.506
1 6 .	3 24	$7\ 688\times10^3$	415	6 022
1 8	3 49	$1\ 182\times10^4$	386	5 779
1 9	3 70	$1\ 494\times10^4$	384	5 885
2 0	4 00	$1\ 868\times10^4$	405	5 993
2 5	5 06	$4\ 619\times10^4$	415	6 069
3 0	6 10	$9\ 558\times10^4$	419	6 057
3 5	7 10	$1\ 771\times10^5$	0 417	6 058

* From Chandrasekhar (1961)

maximum for $\lambda = 2.5$, and finally approaches an asymptotic value of approximately 0.25. The minimum value of α/λ is attained at that value of λ at which the fluid makes the transition from a single vertical cell to a double cell. The oscillatory nature of the α/λ versus λ values seems to be related to the numbers of vertical cells associated with the motion. As the Rayleigh number approaches the point where the optimum motion requires two cells instead of one, the horizontal wavelength of the single cell has a maximum value. Where the transition occurs from two cells to three, the horizontal scale is a (local) minimum. One can perhaps generalize and say that the transition from an odd to an even number of cells is associated with a maximum horizontal scale, whereas the transition from an even to an odd number is accompanied by a minimum horizontal scale. It should be noted that the foregoing statement is a generalization drawn from the small amount of data in Table 1 and may not be correct.

The minimum Rayleigh number occurs at $\lambda = 1.68$, which corresponds to a top temperature of about 6.7° C. The asymptotic value for large λ appears to be 2.83. Why should the fluid be most unstable when the top temperature exceeds 4° C, and, in particular, why does it choose the specific value of $\lambda = 1.68$ as the most preferred value?

The first part of the question seems to have an obvious answer. By adding stable fluid above, one relaxes the boundary condition at the top, and the fluid motion can achieve its optimum form. However, from this argument alone, one might expect the minimum

Rayleigh number to occur when the fluid layer was very deep and the unstable layer was restricted to a small depth near the bottom. In that case the inhibiting effect of the upper boundary would be minimized. However, there are two additional characteristics of the fluid system which are pertinent and tend to reduce the optimum value of λ.

The first of these characteristics is associated with the presence of multiple cells. As the value of λ is increased, the optimum form of the motion is one with more than one cell. The second cell lies completely within the stable fluid and must be driven by (i.e., must draw its energy from) the motion in the unstable layer by means of viscous forces. One might expect the presence of a second cell to be a drain on the energy of the unstable part of the system and that an optimum upper temperature would be one for which the fluid motion had only a single cell in the vertical.

The second pertinent feature of the fluid system is based on the distribution of density of the conductive state. Gravitationally, the fluid from 0° to 4° C is unstable, and the fluid above 4° C is stable. However, when we speak of a gravitationally stable or unstable layer of fluid we are thinking of the relationship of the layer to contiguous layers. In our particular example other considerations must enter because, even though the 5° C layer is locally stable, it is unstable with respect to all layers below 3° C. If there were some way for the 5° C layer to penetrate below the 3° C depth, it would be able to release

a *b*

FIG. 3 —(*a*) The density profile associated with the pure conduction state is sketched for the case with the top temperature between 4° and 8° C. (*b*) The redistributed density profile has the densest fluid at the bottom, the next dense layer above it, etc. There is a discontinuity in slope at a distance $2d - h$ below the upper surface. Below this point two temperatures correspond to each value of the density.

potential energy. We can pose this problem as a quantitative one by the following procedure.

Suppose we redistribute adiabatically the various layers of fluid, so that the densest (4° C) layer is at the bottom and the vertical density profile is gravitationally stable—i.e., the density decreases continuously with height. In doing so, we neglect boundary conditions and look merely at the configuration of minimum potential energy, with the constraint that we preserve the existence of each layer of fluid. If we subtract the potential energy of this redistributed configuration from the potential energy of the actual conductive state, we have a measure of the maximum amount of potential energy "available" to the system by adiabatic redistribution. It should be kept in mind that we are redistributing only the density layers and are ignoring temperature effects and micro-processes. The calculation is simple and straightforward.

It is clear that we can neglect the region of water with temperature greater than 8° C, since the density distribution is the same in the two cases and we are interested only in the difference of potential energies. Hence, consider the conductive state sketched in Figure 3, *a*. The temperature at the top boundary has a value between 4° and 8° C. The symmetric portion of the curve lies in the range $2d-h \leq z \leq h$. (Thus if the top temperature were 8° C, the entire region would be symmetric.) Now for the configuration of minimum potential energy it is clear that the layer of water below $z = 2d-h$ must be turned upside down and placed at the top, the 4° C layer must be at the bottom, and the symmetric layers on either side of the 4° C layer must be combined and placed next to each other, with density decreasing with height. We then get the configuration shown in Figure 3, *b*.

Mathematically, the redistributed density profile can be written down by inspection:

$$\rho = \rho_0\left[1 - \alpha'\left(\frac{z}{2}\right)^2\right], \qquad 0 \leq z \leq 2(h-d), \tag{52a}$$

$$\rho = \rho_0[1 - \alpha'(z - h + d)^2], \qquad 2(h-d) \leq z \leq h, \tag{52b}$$

where $\alpha' = \alpha(\Delta I/d)^2$. The factor $\frac{1}{2}$ appears with z in formula (52*a*) because each value of the density corresponds to two layers in the conductive configuration of Figure 3, *a*, one on either side of 4° C.

Now the vertically integrated potential energy per unit area for Figure 3, *a*, is given by

$$\int_0^h g\rho_0[1 - \alpha'(z-d)^2]\, z\, dz, \tag{53}$$

and the same quantity for Figure 3, *b*, is given by

$$\int_0^{2(h-d)} g\rho_0\left[1 - \alpha'\left(\frac{z}{2}\right)^2\right] z\, dz + \int_{2(h-d)}^h g\rho_0[1 - \alpha'(z-h+d)^2]\, z\, dz. \tag{54}$$

We subtract quantity (54) from quantity (53) for the difference and have, after a simple integration and collection of terms,

$$\frac{\Delta PE}{\text{Unit area}} = g\rho_0\alpha'\left[\frac{(h-d)^4}{6} - d\,\frac{(h-d)^3}{3} + \frac{(h-d)\,d^3}{3} + \frac{1}{6}\right]$$

or

$$\frac{\Delta PE}{\text{Unit area}} = \frac{g\rho_0\alpha' d^4}{3}\left[\frac{(\chi-1)^4}{2} - (\chi-1)^3 + \chi - 1 + \tfrac{1}{2}\right], \tag{55}$$

where $\chi = h/d$.

Maximizing ΔPE with respect to χ, we arrive at

$$\tfrac{2}{3}(\chi-1)^3 - (\chi-1)^2 + \tfrac{1}{3} = 0, \tag{56}$$

with solutions $\chi = 2$, $\chi = 2$, $\chi = \frac{1}{2}$. The maximum occurs at $\chi = 2$ or $h = 2d$, as might have been anticipated.

In summary, the value of the critical Rayleigh number is affected by the presence of the stable fluid in the region above the 4° C layer through three physical features: (*a*) the relaxation of the upper boundary condition would favor a very thick stable layer; (*b*) the increase in "available" potential energy would favor a temperature at the top boundary with a value of 8° C and would not be affected by further deepening of the stable layer; (*c*) the necessity for more than a single cell to form implies that energy must be drawn from the kinetic energy of the unstable layer, and this process favors a layer with the temperature at the top boundary less than 8° C. The complex interaction of these three processes is included in the stability analysis and indicates an optimum top temperature of about 6.7° C.

IV. FINITE AMPLITUDE METHOD AND SOLUTION FOR $\lambda = 2$

Thus far we have treated the first-order equations. Higher-order equations can be derived from the set (20)–(23) when the expansions (26) are substituted. The zero-order terms are time-independent, and it can be shown that the higher-order quantities will also not involve time. The pertinent equations are

$$\epsilon^2: \mathfrak{L}T_1 = R_1(1-\lambda z)\nabla_1^2 T_0 + \nabla^4 h_{00} - \frac{\lambda}{2}\nabla_1^2 T_0^2 - \frac{R_0}{\sigma}L_{00}, \tag{57a}$$

$$\nabla^2 T_1 = R_0 w_1 + R_1 w_0 + h_{00}, \tag{57b}$$

$$\nabla^2\nabla_1^2 v_1 = -\nabla^2\frac{\partial^2 w_1}{\partial y \partial z} + \frac{\partial^2}{\partial x^2}(v_0 - \nabla v_0) - \frac{\partial^2}{\partial x \partial y}(v_0 \cdot \nabla u_0), \tag{57c}$$

$$\nabla^2\nabla_1^2 u_1 = -\nabla^2\frac{\partial^2 w_1}{\partial x \partial z} + \frac{\partial^2}{\partial y^2}(v_0 \cdot \nabla u_0) - \frac{\partial^2}{\partial x \partial y}(v_0 \cdot \nabla v_0). \tag{57d}$$

$$\begin{aligned}\epsilon^3: \mathfrak{L}T_2 &= R_2(1-\lambda z)\nabla_1^2 T_0 + R_1(1-\lambda z)\nabla_1^2 T_1 \\ &+ \lambda\left[(w_0T_0)_m z - \int_0^z \langle w_0 T_0\rangle dz^1\right]\nabla_1^2 T_0 + \nabla^4\{[\langle w_0T_0\rangle - (w_0T_0)_m]w_0\} \\ &+ \nabla^4(h_{01}+h_{10}) - \lambda\nabla_1^2 T_1 T_0 - \frac{R_0}{\sigma}(L_{01}+L_{10}) - \frac{R_1}{\sigma}L_{00},\end{aligned} \tag{58a}$$

$$\nabla^2 T_2 = R_0 w_2 + R_1 w_1 + R_2 w_0 + [\langle w_0 T_0\rangle - (w_0T_0)_m]w_0 + h_{01} + h_{10}, \tag{58b}$$

$$\nabla^2\nabla_1^2 v_2 = -\nabla^2\frac{\partial^2 w_2}{\partial y \partial z} + \frac{\partial^2}{\partial x^2}(v_0 \cdot \nabla v_1 + v_1 \cdot \nabla v_0) - \frac{\partial^2}{\partial x \partial y}(v_0 \cdot \nabla u_1 + v_1 \cdot \nabla u_0), \tag{58c}$$

$$\nabla^2\nabla_1^2 u_2 = -\nabla^2\frac{\partial^2 w_2}{\partial x \partial z} + \frac{\partial^2}{\partial y^2}(v_0 \cdot \nabla u_1 + v_1 \cdot \nabla u_0) - \frac{\partial^2}{\partial x \partial y}(v_0 \cdot \nabla v_1 + v_1 \cdot \nabla v_0), \tag{58d}$$

where $h_{ij} = v_i \cdot \nabla T_j - (\partial/\partial z)\langle w_i T_j\rangle$ and equivalent use of i, j applies to L_{ij}.

To solve for T_1, we could proceed formally as follows: Equation (57a) is an inhomogeneous equation for T_1. A necessary and sufficient condition for a solution to this equation to exist (Ince 1926) is that

$$\int_0^1 \tilde{T}_0\left[R_1(1-\lambda z)\nabla_1^2 T_0 + \nabla^4 h_{00} - \frac{\lambda}{2}\nabla_1^2 T_0^2 - \frac{R_0}{\sigma}L_{00}\right]dz = 0,$$

where $\tilde{T}_0$ is the adjoint function defined by the equation

$$\int_0^1 \tilde{T}_0 \mathfrak{L} T_0 dz = \int_0^1 T\tilde{\mathfrak{L}}\tilde{T}_0 dz = 0,$$

which serves also to define the operator $\tilde{\mathfrak{L}}$.

The necessary and sufficient condition yields the following expression:

$$R_1\int_0^1 \tilde{T}_0(1-\lambda z)\nabla_1^2 T_0 dz = \int_0^1\left[\tilde{T}_0\frac{\lambda}{2}\nabla_1^2 T_0^2 + \frac{R_0}{\sigma}\tilde{T}_0 L_{00} - \tilde{T}_0\nabla^4 h_{00}\right]dz. \tag{59}$$

Once R_1 is evaluated in this manner, the remaining part of the right-hand side of equation (57a) provides the forced solution T_1 and the procedure is straightforward.

A remaining arbitrariness is due to the fact that $\mathfrak{L}T_i = 0$ can be satisfied by an arbitrary multiple of T_0. We can eliminate this arbitrariness by the following procedure: Normalize T_0 so that $(T_0^2)_m = 1$ and impose the condition that $(T_0 T)_m = \epsilon$, i.e., that

$(T_i T_0)_m = 0$ for $i > 0$. Then all the amplitude of the T_0 term is put into ϵ. This serves to give specific meaning to ϵ, as well as to remove the arbitrariness.

Once T_1 has been determined, u_1, v_1, w_1 can also be evaluated from the set (57); R_2, T_2, u_2, v_2, w_2, etc., can then be evaluated by repeating the procedure.[6] For our case the operator and boundary conditions render the problem self-adjoint, so that $\tilde{T}_0 \equiv T_0$ and $\tilde{\mathfrak{L}} \equiv \mathfrak{L}$.

If T_0 were known exactly, we could proceed as outlined. However, it will be seen that, since T_0 is known only approximately, the method breaks down. Limited finite amplitude results can, however, be derived by the present technique. We proceed with the case where the horizontal spatial dependence is one-dimensional, i.e., $\partial/\partial y \equiv 0$.

a) Two-dimensional Cells (Rolls)

The normalized approximate solution for T_0 for the case 0°–8° C is

$$T_0 = (A_1 \sin \pi z + A_2 \sin 2\pi z) \cos \pi a x\,, \tag{60a}$$

where $A_1 = 1.943$, $A_2 = 0.474$, so that $(T_0^2)_m = 1$.

The remaining first-order variables can be derived from equations (21), (22), and (23), with the non-linear terms neglected. This gives

$$w_0 = -\frac{\pi^2}{R_0}[(a^2+1)A_1 \sin \pi z + (a^2+4)A_2 \sin 2\pi z] \cos \pi a x\,, \tag{60b}$$

$$u_0 = \frac{\pi^2}{aR_0}[(a^2+1)A_1 \cos \pi z + 2(a^2+4)A_2 \cos 2\pi z] \sin \pi a x\,, \tag{60c}$$

$$v_0 = 0\,. \tag{60d}$$

Substituting the zero-order variables in equation (57*a*) and proceeding as outlined, we obtain

$$\nabla^4 h_{00} = \frac{3\pi^7 A_1 A_2}{4R_0}[(9+4a^2)^2 \sin 3\pi z - 3(1+4a^2)^2 \sin \pi z] \cos 2\pi a x\,,$$

$$\frac{R_0}{\sigma} L_{00} = \frac{3\pi^7}{2R_0\sigma} A_1 A_2 (a^2+1)(a^2+4)(\sin 3\pi z - 3 \sin \pi z) \cos 2\pi a x\,,$$

$$\nabla_1^2 T_0^2 = -\pi^2 a^2 [A_1^2(1-\cos 2\pi z) + 2A_1A_2(\cos \pi z - \cos 3\pi z) + A_2^2(1-\cos 4\pi z)] \cos 2\pi a x\,.$$

When these are substituted in the right-hand side of equation (57*a*) and the equation is multiplied by T_0 and integrated, the result is

$$R_1 = 0 \tag{61}$$

because of the orthogonality of $\cos \pi a x$ and $\cos 2\pi a x$.

With R_1 known, we can solve equation (57*a*) approximately for T_1. This is done by substituting $\nabla_1^2 = -4\pi^2 a^2$ (since the horizontal dependence is uniformly $\cos 2\pi a x$) and letting T_1 be expressed in terms of the Fourier series:

$$T_1 = \sum_1^{\infty} B_n \sin n\pi z\,.$$

[6] The method outlined here is the correct procedure for the problem with any homogeneous boundary conditions. The procedure outlined in an earlier paper (Malkus and Veronis 1958) is incorrect, but the computed results are valid because the method employed coincides with the present form when the operator is self-adjoint—the only case actually computed.

To determine the B_n's we multiply the equation by $\sin r\pi z$ and integrate. The procedure gives rise to an infinite set of inhomogeneous equations. It turns out that the truncated 3×3 matrix is sufficient to give results correct to 1 per cent. We find

$$T_1 = \sum_1^3 B_n \sin n\pi z \cos 2\pi a x , \tag{62}$$

where $B_1 = -15.08\, \pi/8a^2R_0$, $B_2 = -5.077\pi/8a^2R_0$, $B_3 = -0.6111\pi/8a^2R_0$. The quantities w_1 and u_1 can be computed from equations (57). We can then proceed to (58*a*) for the next higher-order quantities.

The first information regarding amplitude can be deduced from the value of R_2, which can be determined at this point. Since u_i, v_i, w_i, T_i, and R_i are all known for $i = 0, 1$, the right-hand side of equation (58*a*) is known. Hence the procedure outlined in the paragraphs following equation (58*d*) will yield R_2. That is, we multiply the right-hand side of equation (58*a*) by T_0 and average. The quantity R_2 is then expressed in terms of definite integrals of known quantities. The computation is very tedious and will not be reproduced here. The result is

$$R_2 = -0.00366 . \tag{63}$$

We return to equation (26) and note that, to the second order (since $R_1 = 0$),

$$R = R_0 + \epsilon^2 R_2$$

or

$$\epsilon^2 = \frac{R - R_0}{R_2} . \tag{64}$$

Hence, since $\epsilon^2 > 0$ and $R_2 < 0$, it is necessary that $R < R_0$. In other words, the solution which we have found is valid for subcritical Rayleigh numbers. If disturbances of finite amplitude are present which enable this roll solution to form, a motion field would be established for values of R less than R_0. This type of finite amplitude instability was also derived for convection in a rotating system (Veronis 1959). However, in that case the values of the parameters necessary for the finite amplitude instability did not correspond to those available in the laboratory. In the present case, the experiment can be carried out.

The non-dimensional form of the heat flux expression (9) to the second order is

$$\frac{H}{-\kappa(\Delta T/d)} = 1 - \frac{\epsilon^2}{R}(w_0 T_0)_m = 1 + 1.33 \frac{R_0 - R}{R} . \tag{65}$$

This result is plotted in Figure 4. The heat transport increases indefinitely as $R \to 0$. It is clear that the second-order approximation must break down at some point and one must go to higher-order terms as $(R_0 - R)/R$ becomes larger. The curve must eventually turn up again. Possible curves are dashed into the figure. The farther to the right the turning up occurs, the lower the Rayleigh number, and the more dramatic will be the jump in heat transport when the finite amplitude instability sets in.

As described in an earlier paper (Veronis 1959), experimentally the behavior of the system for R near R_0 depends on the manner in which the Rayleigh number is varied and on the background noise. If R is increased from $R = 0$, the heat transport could increase to a value larger than the conduction value for *any* fixed value of R between $R_{\min}$[7] and R_0, depending on the amplitude of the noise. If the latter is infinitesimal, the conduction line will obtain until $R = R_0$. Then H will jump to the maximum allowed value, and an increase in R is necessary for any further increase in H. Jumps in heat transport for values between R_0 and $R_{\min}$ depend on the amplitude of the noise. If R

[7] $R_{\min}$ is the point where the dashed curve attains a minimum.

is decreased from a supercritical value, the value of H for a given R will always be the maximum possible, i.e., motions will always exist for $R_{\min} \leq R \leq R_0$.

b) Hexagonal Cells

When the horizontal plan form is hexagonal, a horizontal asymmetry is introduced. The vertical dependence is, of course, not symmetric (cf. Fig. 2). The asymmetry for hexagonal cells provides some new and interesting results. In the first place, it will be shown that $R_1 \neq 0$. This result is interesting because a non-vanishing R_1 makes a finite amplitude instability possible, regardless of the sign of R_2. This rather surprising result can be seen immediately from the expansion of R. To the first order we have

$$R - R_0 = \epsilon R_1 . \tag{66}$$

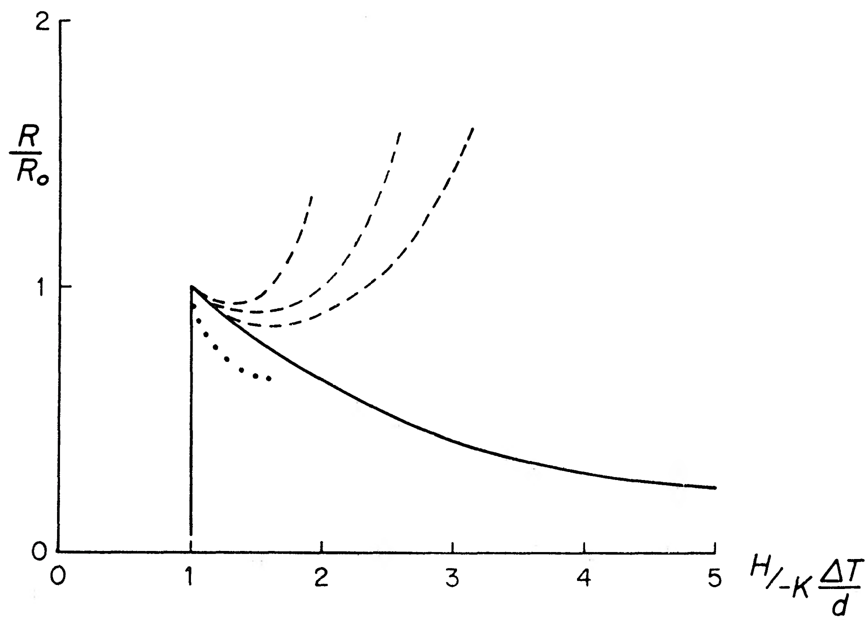

FIG. 4.—The non-dimensional heat transport is plotted as a function of R/R_0 The solid line is the curve for roll solutions to order ϵ^2. The dashed curves are possible roll solutions with higher-order terms. For hexagons (*dotted curve*) the results show that the curve is tangent to the conduction line.

If $R_1 \gtrless 0$, then $\epsilon \lessgtr 0$ requires that $R < R_0$. Thus it is always possible for a solution to exist for subcritical R. Higher-order terms cannot alter this result because equation (66) is always the dominant relation in some restricted range of $R - R_0$.

The possibility for a finite amplitude instability as given by equation (66) is explicitly associated with the asymmetry of the problem. In the case of rolls, the horizontal plan form is symmetric, and, at any given point, the sign of the vertical velocity, for example, can always be altered by translating the reference axes. This symmetry is reflected in the fact that only ϵ^{2n} terms appear in the R expansion. Thus a subcritical finite amplitude solution for rolls is possible only when R_2 has the appropriate sign. For hexagons the sign of ϵ is an added degree of freedom, and a subcritical finite amplitude instability is always possible and should occur, provided that the white noise background has sufficient amplitude. This result may serve to explain the occurrence of hexagons in the Bénard type of experiments where the top boundary is a free surface. Since a finite amplitude solution is possible for subcritical R, it would be the preferred solution according to the relative stability criterion of Malkus and Veronis (1958).

The second interesting aspect of the hexagonal case is that the non-vanishing of R_1 creates a problem for extending the solution to obtain R_2. The difficulty is associated with the fact that we have only approximate solutions for the stability problem. (We would have been confronted with this difficulty in the case of rolls, had we attempted to go beyond the R_2 calculation.)

The normalized form of T_0 for hexagons is

$$T_0 = \phi(A_1 \sin \pi z + A_2 \sin 2\pi z), \qquad (T_0^2)_m = 1$$

$$\phi = 2 \cos \frac{\sqrt{(3)}\pi a x}{2} \cos \frac{\pi a y}{2} + \cos \pi a y, \tag{67a}$$

$$A_1 = 1.1218, \qquad A_2 = 0.2736.$$

The corresponding velocities are

$$w_0 = -\frac{\pi^2}{R_0} \phi [(a^2+1) A_1 \sin \pi z + (a^2+4) A_2 \sin 2\pi z], \tag{67b}$$

$$u_0 = \frac{\pi^2 \sqrt{3}}{R_0 a} \sin \frac{\sqrt{(3)}\pi a x}{2} \cos \frac{\pi a y}{2} [(a^2+1) A_1 \cos \pi z + 2(a^2+4) A_2 \cos 2\pi z], \tag{67c}$$

$$v_0 = \frac{\pi^2}{R_0 a} \left[\cos \frac{\sqrt{(3)}\pi a x}{2} \sin \frac{\pi a y}{2} + \sin \pi a y\right] \times [(a^2+1) A_1 \cos \pi z + 2(a^2+4) A_2 \cos 2\pi z]. \tag{67d}$$

Proceeding with the calculation of the inhomogeneous terms in equation (57*a*), we find

$$\mathfrak{L}T_1 = -\pi^2 a^2 R_1 (1-2z) \phi (A_1 \sin \pi z + A_2 \sin 2\pi z) + \left[\sum_1^4 a_n \sin n\pi z\right]\phi + \left[\sum_1^4 b_n \sin n\pi z\right]\psi + \left[\sum_1^4 c_n \sin n\pi z\right]\chi, \tag{68a}$$

where the a_n, b_n, and c_n's are known constants (independent of R_1) and

$$\psi = 2 \cos \sqrt{(3)}\pi a x \cos \pi a y + \cos 2\pi a y, \qquad \nabla_1^2 \psi = -4\pi^2 a^2 \psi, \tag{68b}$$

$$\chi = 2 \cos \frac{\sqrt{(3)}\pi a x}{2} \cos \frac{3\pi a y}{2} + \cos \sqrt{(3)}\pi a x, \qquad \nabla_1^2 \chi = -3\pi^2 a^2 \chi. \tag{68c}$$

The functions ψ and χ are harmonics of the basic hexagonal plan form, ϕ.

The difficulty which arises is associated with the coefficients of ϕ in equation (68*a*). (The particular solutions resulting from the ψ and χ expressions can be deduced in the usual manner and lead to no difficulties.) Let us suppose that R_1 has been evaluated as before In fact, if one proceeds as before, one finds

$$R_1 = 1.4\pi. \tag{69}$$

Now the problem is to compute that part of T_1 that is proportional to ϕ. Continuing with our approximation procedure, we substitute

$$T_1 = \sum_1^\infty B_n \sin n\pi z \phi \tag{70}$$

in equation (68*a*) (with the ψ and χ terms deleted) and then multiply by sin $r\pi z$ and integrate from $z = 0$ to $z = 1$. We end up with the infinite set of inhomogeneous equations,

$$\begin{aligned}
\frac{-\pi^6(1+\alpha^2)^3}{4\alpha^2 R_0} B_1 + \tfrac{8}{9}B_2 + 0 + \tfrac{16}{225}B_4 + \ldots &= m_1,\\
\tfrac{8}{9}B_1 - \frac{\pi^6(4+\alpha^2)^3}{4\alpha^2 R_0} B_2 + \tfrac{24}{25}B_3 + 0 + \ldots &= m_2,\\
0 + \tfrac{24}{25}B_2 - \frac{\pi^6(9+\alpha^2)^3}{4\alpha^2 R_0} B_3 + \tfrac{48}{49}B_4 + \ldots &= m_3,\\
\tfrac{16}{225}B_1 + 0 + \tfrac{48}{49}B_3 - \frac{\pi^6(16+\alpha^2)^3}{4\alpha^2 R_0} B_4 + \ldots &= m_4,
\end{aligned} \tag{71}$$

where the m_i's are known constants and include the value of R_1.

The determinant made up of the coefficients of the left-hand side of equations (71) is precisely the determinant that was equated to zero to yield the R_0 versus α^2 relation for the stability problem. The fact that the 4×4 determinant does not vanish arises from the original approximation, where only the 2×2 determinant was used. However, this means that solving for the B_i's above is possible only because of the small residual errors which were neglected originally. As might be expected, the method leads to absurd results.

The difficulty can be removed by the following procedure: We rewrite T_0 so that only that part of it which has the form $A_1\phi$ sin πz is normalized, i.e., $A_1 = 2/\sqrt{3}$. The amplitude $A_2 = 0.282$ is then determined from the stability problem. Now ϵ is interpreted as the amplitude of ϕ sin πz. Hence none of the T_i's, $i > 0$, contain a term of the form ϕ sin πz, because $(\phi \sin \pi z T)_m = \epsilon$ and this automatically implies that all T_i's with $i > 0$ are orthogonal to ϕ sin πz. The procedure is therefore altered because R_1 must now be evaluated so as to absorb all the amplitude of terms of the form ϕ sin πz on the right-hand side of equation (68*a*). We shall therefore substitute

$$T_1 = \sum_2^\infty B_n \sin n\pi z$$

in equation (68*a*) (note that $B_1 \equiv 0$), and we therefore force all the amplitude of ϕ sin πz to be absorbed into R_1. Hence, after multiplying by sin $r\pi z$ and integrating, we obtain a new set of linear inhomogeneous equations of the form

$$\begin{aligned}
\frac{8A_2}{9R_0} R_1 + \tfrac{8}{9}B_2 + 0 + \tfrac{16}{225}B_4 + \ldots &= P_1,\\
\tfrac{8}{9}\frac{A_1}{R_0} R_1 - \frac{(4+\alpha^2)^3}{2}\pi^6 B_2 + \tfrac{24}{25}B_3 + 0 + \ldots &= P_2,\\
\tfrac{24}{25}\frac{A_2}{R_0} R_1 + \tfrac{24}{25}B_2 - \frac{(9+\alpha^2)^3}{2}\pi^6 B_3 + \tfrac{48}{49}B_4 + \ldots &= P_3,\\
\frac{16A_1}{225R_0} R_1 + 0 + \tfrac{48}{49}B_3 - \frac{(16+\alpha^2)^3}{2}\pi^6 B_4 + \ldots &= P_4,
\end{aligned} \tag{72}$$

where the P_i's are known constants. Note that the result will give R_1 and the form of the ϕ part of T_1 simultaneously.

The truncated 4×4 set is sufficient for our purposes, and we derive the results

$$R_1 = 1.27\pi\,, \qquad B_2 = 1.28\,\frac{\pi}{2\,a^2R_0}\,, \qquad B_3 = 0.488\,\frac{\pi}{2\,a^2R_0}\,, \qquad B_4 = 0.0658\,\frac{\pi}{2\,a^2R_0}\,.$$

The value of R_1 differs from that computed previously (69). However, it has a different meaning, since it determines the amplitude of $\phi \sin \pi z$ instead of the amplitude of the entire T_0 term. If we compare the two methods by computing the amplitude of $\phi \sin \pi z$ in the two cases, we find that the amplitudes differ by about 9 percent. It should be noted that this result is based on eigenfunctions which gave the critical Rayleigh number with an error of considerably less than 1 per cent. Thus the error appears to mount up in higher-order calculations if one applies the method originally proposed. The crucial point is, of course, that one cannot continue the solution to higher-order terms with the first method.

A suitable program seems to be the following: Decide a priori (if possible) to what order, j, the calculation will be made and then proceed by the second method up to the R_j calculation. Make the final R_j calculation according to the old method, which is much simpler because it involves only those terms which sufficed for the stability problem. There will, of course, be an error in the value of R_j, but at least it will have been minimized by the correct procedure prior to the R_j evaluation. The reason for making the last step approximately is that a number of terms which must now be kept to proceed according to the revised method can be dropped if the old method is used. If feasible, the new method should, of course, be used for all calculations.

For the present calculation, one proceeds with the evaluation of those parts of T_1 which have horizontal plan forms ψ and χ. Substituting

$$T_1 = \psi \sum_1^4 C_n \sin n\pi z \qquad \text{and} \qquad T_1 = \chi \sum_1^4 D_n \sin n\pi z\,,$$

one now computes

$$\begin{aligned} C_1 &= -5.32\,\frac{\pi}{8a^2R_0}\,, & D_1 &= -14.6\,\frac{\pi}{6\,a^2R_0}\,, \\ C_2 &= -2.02\,\frac{\pi}{8a^2R_0}\,, & D_2 &= -4.22\,\frac{\pi}{6\,a^2R_0}\,, \\ C_3 &= -1.13\,\frac{\pi}{8\,a^2R_0}\,, & D_3 &= 0.0128\,\frac{\pi}{6\,a^2R_0}\,, \\ C_4 &= -0.0196\,\frac{\pi}{8a^2R_0}\,, & D_4 &= 0.0466\,\frac{\pi}{6\,a^2R_0}\,. \end{aligned} \tag{73}$$

The amplitudes C_4, D_3, and D_4 are actually negligible. They have been included only as checks on the truncation.

We can compute w_1, u_1, and v_1, from equations (57). There is little point in continuing with an outline of the actual computation. It is necessary to note only that the terms h_{01}, h_{10}, L_{01}, L_{10}, etc., on the right-hand side of equation (54a) can now be computed. It is then possible to evaluate R_2. One calculates

$$(R_2)_{\text{hex}} = -0.00201\pi^2\,. \tag{74}$$

Hence, we have to the second order,

$$-0.00201(\epsilon\pi)^2 + 1.27(\epsilon\pi) + R_0 - R = 0\,,$$

the solution of which is approximately

$$\epsilon = \frac{R - R_0}{1.27\pi}[1 + 0.000126(R - R_0)]. \tag{75}$$

The useful qualitative aspect of this result has already been pointed out, viz., that it is possible for a solution to exist for $R < R_0$. A second important qualitative feature of equation (75) is that, for finite amplitude subcritical motions, $\epsilon < 0$, i.e., the motion at the center of the hexagonal cell is upward (because $w_0 < 0$, hence $\epsilon w_0 > 0$).

A third result of interest is that the R/R_0 versus $H/-\kappa(\Delta T/d)$ curve is tangent to the conduction line at the critical point and then turns down and to the right (dotted line in Fig. 4). This is in marked contrast to the result for rolls, where there is an abrupt departure from the conduction line for all values of $R_0 - R > 0$ and is a result of the asymmetry which gives a non-zero R_1. However, here again we are confronted with the problem that the region in which the last two results are applicable may not be observable experimentally. It is necessary to go to an order which allows the curve to turn up again in the R/R_0 versus $H/-\kappa(\Delta T/d)$ diagram. Therefore, the only useful information that we obtain in this case is that a finite amplitude solution exists for subcritical R.

V. SUMMARY AND CONCLUSIONS

The method used for the solution of the finite amplitude motions is pivoted about the solution to the linear stability problem. A technique is described that can be used to derive the finite amplitude results when the solution to the stability problem is known only approximately. One expands the variables and the external (eigen) parameter, R, in powers of a small parameter ϵ. The coefficients, R_j, of ϵ_j must be determined. To proceed, one expands the first-order variables in terms of a complete orthogonal set. The resulting set of homogeneous equations and boundary conditions determines the eigenvalue and the approximate (truncated) set of eigenfunctions. The set of equations which form the coefficient of ϵ_j have products of the zero-order variables as known inhomogeneous terms. In order to reduce the procedure to a consistent one, we normalize the first (or some other) component function of the complete orthogonal set and identify ϵ with the amplitude of that component. The higher-order terms then do not contain that component. R_1 is evaluated so as to balance the amplitude of the normalized component in the non-linear inhomogeneous forcing terms. The procedure is actually quite similar to that described by Malkus and Veronis (1958), but an alteration is introduced because the first-order problem is solved only approximately.

The results indicate that when the bottom of a layer of water is maintained at 0° C temperature and the top at >4° C, a finite amplitude instability should set in at values of the Rayleigh number below the critical value given by linear stability theory. Furthermore, a general result of the expansion indicates that, for a system with built-in asymmetries, a finite amplitude instability is always possible. No physical justification has been set forth for this last conclusion. However, a simple physical argument can be produced for the occurrence of a finite amplitude instability in the problem considered. Any finite amplitude motion which mixed water above and below the 4° C layer would create a deeper layer of water that would be more unstable gravitationally than the corresponding unstable layer in the conduction state. Hence a subcritical finite amplitude instability may occur if the white noise background has sufficient amplitude.

An experimental investigation by Furumoto and Rooth has been directed toward establishing the occurrence or absence of a finite amplitude instability. Thus far, no experimental evidence is available to establish whether or not the system is unstable at subcritical Rayleigh numbers.

The particular method described in the paper has limited usefulness here because the H versus R relation is derived for a subcritical R-range, where the mathematical solution is probably unstable. That is, since the heat transport increases for decreasing Rayleigh number, at some value of the Rayleigh number the H versus R curve must turn back up, so that there exists another (probably preferred) value of H for a given subcritical R.

The calculation must be carried to higher orders—possibly the sixth order—before the results can be compared with experiment. However, the same method can be applied to other physical problems in which subcritical motions do not occur. In particular, the finite amplitude motions for flow between cylinders of opposite rotation can be analyzed by the present method, and one ought to be able to deduce second-order results which can be compared with experiment.

It is a pleasure to record my thanks to L. N. Howard, W. V. R. Malkus, and E. A. Spiegel for their help, interest, and encouragement and to the Office of Naval Research, which provided financial support during the course of this research effort. This is Contribution No. 1243 from the Woods Hole Oceanographic Institution.

REFERENCES

Chandrasekhar, S. 1954, *Mathematika*, **1**, 5.
———. 1961, *Hydrodynamic and Hydromagnetic Stability* (Oxford: Oxford University Press).
Ince, E. L. 1926, *Ordinary Differential Equations* (New York: Dover Publications), p. 214.
Jeffreys, H., and Jeffreys, B. S 1946, *Methods of Mathematical Physics* (Cambridge: Cambridge University Press).
Malkus, W. V. R., and Veronis, G. 1958, *J. Fluid Mech.*, **4**, 3
Taylor, G. I. 1923, *Phil. Trans A*, Vol. **223**.
Veronis, G. 1959, *J. Fluid Mech*, **5**, 3.